01 Aug 2008

Closed-form Expressions for Determining Approximate PMC Boundaries Around an Aperture in a Metal Cavity Wall

Francesco de Paulis

Yaojiang Zhang
Missouri University of Science and Technology, zhangyao@mst.edu

Jun Fan
Missouri University of Science and Technology, jfan@mst.edu

Jason A. Mix

et. al. For a complete list of authors, see https://scholarsmine.mst.edu/ele_comeng_facwork/922

Recommended Citation

F. de Paulis et al., "Closed-form Expressions for Determining Approximate PMC Boundaries Around an Aperture in a Metal Cavity Wall," *Proceedings of the IEEE International Symposium on Electromagnetic Compatibility, 2008*, Institute of Electrical and Electronics Engineers (IEEE), Aug 2008.
The definitive version is available at https://doi.org/10.1109/ISEMC.2008.4652122

Closed-Form Expressions for Determining Approximate PMC Boundaries around an Aperture in a Metal Cavity Wall

Francesco de Paulis, Yaojiang Zhang, Jun Fan

EMCLab, Missouri University of Science and Technology,
Rolla, MO, USA

Jason Mix, Xiaopeng Dong, Daniel Hua, Kevin Slattery

Intel Corporation,
Portland, OR, USA

***Abstract* — Modern electronic systems may use mixed RF/digital technologies to achieve various functionalities, which leads to various intra-system interference problems including the RF interference from noisy digital circuits to sensitive RF receivers, especially when the overall system is contained in a metal enclosure. A fast method based on a cavity formulation can be used to estimate the internal noise coupling mechanisms inside the enclosure. This method assumes that only the TM_{z0} mode exists inside the enclosure, i.e., the electric field along the z-direction is constant. The cavity formulation fails in the region adjacent to an aperture in an enclosure wall, since the aperture introduces higher order modes. The developed closed-form expressions compute the E_z-field variation along the z-direction. Thus, they can be used to estimate the breakpoint where the cavity method is no longer effective.**

Keywords – Perfect Magnetic Conductor (PMC), Electric field variation, Closed-form expressions, Cavity method, RF interference

I. Introduction

Modern electronic system provides a lot of functionalities by integrating various sub-systems. These sub-systems or blocks are often very close to each other since the dimensions of the overall system are getting smaller and smaller. Therefore, interference among these blocks becomes a critical issue. Especially for compact mixed RF/digital systems where wireless technologies are used in addition to high-speed digital circuits, digital noise which is relatively high in magnitude could significantly affect the RF receivers that are extremely sensitive, causing serious performance issues.

Since these systems are usually enclosed in a metal chassis for reducing radiations and improving immunity, noise coupling mechanisms inside a metal enclosure need to be taken into account during the design process of an electronic system.

An accurate analysis can be performed using 3D simulation tools, but it is usually time-consuming and thus impractical for engineering applications.

A much faster alternative is to use a tool based on the cavity formulation that significantly reduces the complexity of the problem by utilizing closed-form expressions [1]. In this method, the z-directional dimension is assumed to be small enough so that only the TM_{z0} modes exist. Further, the geometry under modeling is assumed to be a cavity with either PEC or PMC conditions at its boundaries, so that fields can be expressed as a series of resonant modes (Eigen values).

If the geometry under modeling is relatively complex but it still can be divided into multiple cavities, the fast approach can be applied by individually modeling every cavity and then connecting all of them together using a segmentation method [2-3].

This method should be carefully used since it fails when the boundaries of the physical structure under modeling are neither PEC nor PMC boundaries. One example is an enclosure with an aperture. The 2D cavity formulation assumes that the E-field along the third dimension, the z-direction is constant, and this is true for a simple empty enclosure, provided that the height is small enough compared to the length and width so that only zero-order mode can be excited along this direction.

An aperture in a wall of the enclosure can significantly modify the characteristics in the region adjacent to the aperture, generating an E_z-field component that is not constant. The segmentation method is then applied to divide the geometry into multiple parts. The regions far enough from the aperture can still be simulated using the cavity formulation, while the aperture region can be modeled using a full-wave method. When the segmentation approach is used, the interface between the two connecting geometries has to be a PMC boundary. The breakpoint between the cavity and the aperture regions shall be selected so that the PMC boundary condition is satisfied.

This paper presents some closed-form expressions that give the percentage of the E_z-field variation along the z-direction when the observation point is moving away from the aperture edge. By using these expressions, the breakpoint can be carefully chosen without violating the assumption used in the segmentation method. Further, the effects of a given aperture size and location on the field distribution in a metal enclosure can be studied with these expressions

II. Problem Description

The E_z-field within a cavity is constant along the z-direction and the E_x and E_y components can be neglected, when the z-directional dimension of the cavity is very small and only the TM_{z0} modes exist. However, when there's an aperture in the wall of the cavity, the E_x and E_y components can exit, and the E_z-field can no longer be considered constant along the z-direction in the regions adjacent to the aperture.

A cavity formulation for impedance computation that assumes a constant E_z-field along the z-direction can start to

978-1-4244-1699-8/08/$25.00 ©2008 IEEE

fail in the case of cavity with an aperture. An expression that approximates the E_z-field variation can be helpful to calculate a breakpoint beyond which the cavity formulation cannot be used anymore. A useful expression should be a function of several parameters that affect the E_z-field variation, such as aperture dimensions, frequency, and aperture position, etc.

A. Test Case Overview

The geometry under study is shown as in Fig. 1. As a reference, a simple empty cavity surrounded by metal walls is investigated first.

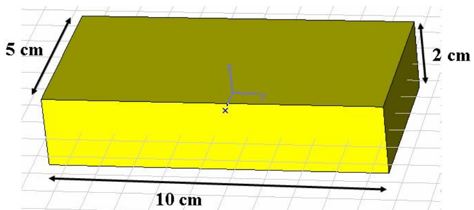

Fig.1. Empty enclosure surrounded by metal walls.

The resonant (modal) frequencies, which relate the physical dimensions (a=10cm, b=5cm, c=2cm) to the electrical behavior of the cavity, are given in (1):

$$f_{mnl} = \frac{c}{2\pi\sqrt{\mu_r \varepsilon_r}} \sqrt{\left(\frac{m\pi}{a}\right)^2 + \left(\frac{n\pi}{b}\right)^2 + \left(\frac{l\pi}{d}\right)^2} \qquad (1)$$

The resulting resonant frequencies for the cavity with the dimensions shown in Fig. 1 are listed in Table 1.

TABLE I
RESONANT FREQUENCIES OF A RECTANGULAR CAVITY

Mode	Frequency (GHz)
TM_{110}	3.35
TM_{210}	4.24
TM_{310}	5.41
TM_{120}	6.18
TM_{220}	6.71
TM_{410}	6.71
TM_{320}	7.5
TM_{101}	7.65
TM_{510}	8.08
TM_{011}	8.08
TM_{201}	8.08
TM_{111}	8.22
TM_{420}	8.49
TM_{211}	8.62
TM_{301}	8.75

The first seven resonances correspond to the TM_{z0} modes, so the electric filed can be assumed constant along the z-direction. Fig. 2 shows the E_z-field as a function of x and y for the TM_{310} mode from a top and side view. As clearly demonstrated in the side view, the variation of the electrical field along the z direction is negligible.

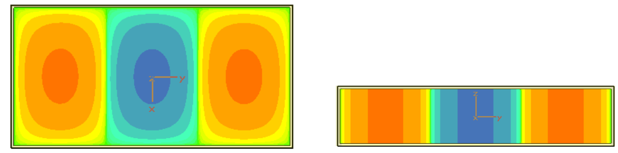

(a) (b)

Fig.2. Field distribution in the cavity at 5.41 GHz: (a) top, and (b) side view.

Starting from f = 7.65 GHz (the resonant frequency of the TM_{101} mode), non-zero modes can be excited along the z-direction. Therefore the cavity method with the TM_{z0} mode assumption will not be able to accurately predict impedance values at the frequencies higher than 7.65 GHz.

When there is an aperture in the wall of the enclosure, the E-field in the adjacent region has all possible components. Therefore, even when frequency is below 7.65 GHz, the E_x and E_y fields can be present in the proximity of the aperture. At the same time, the E_z-field is no longer constant along the z-direction in this adjacent region.

B. E-field behavior in a cavity with an aperture

As an example, an aperture is added to the top wall of the enclosure shown in Fig. 1. Fig. 3a and 3b show the side view of the E_x and E_y components, respectively, at a frequency of 3.35GHz, the resonant frequency of the TM_{110} mode. As clearly demonstrated in these two figures, the E_x an E_y components are no longer negligible adjacent to the aperture.

Fig. 4 and Fig. 5 show the ratios of E_x/E_z and E_y/E_z as a function of the z-coordinate at eight different locations. Along the lines P_4 and P_5, when position is close to the aperture (z > 0.5 cm), higher E_x/E_z and E_y/E_z ratios can be observed. The E_x and E_y components could be close to the E_z component in magnitude (i.e., E_x/E_z and E_y/E_z ratios are close to one).

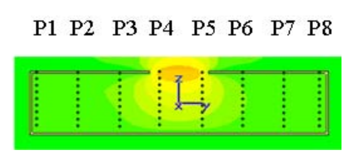

(a)

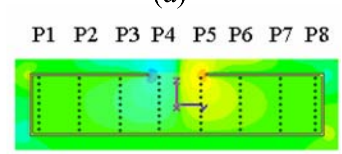

(b)

Fig.3. (a)E_x, and (b) E_y field components at 3.35 GHz.

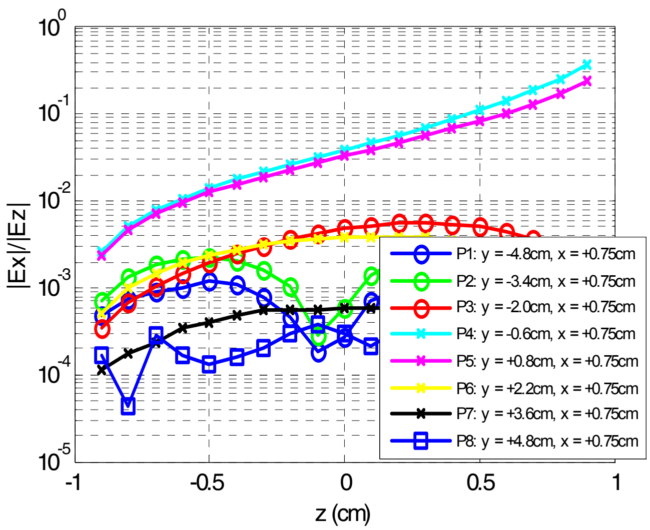

Fig.4. $|E_x|/|E_z|$ ratio as a function of z at 3.35 GHz for the 8 locations.

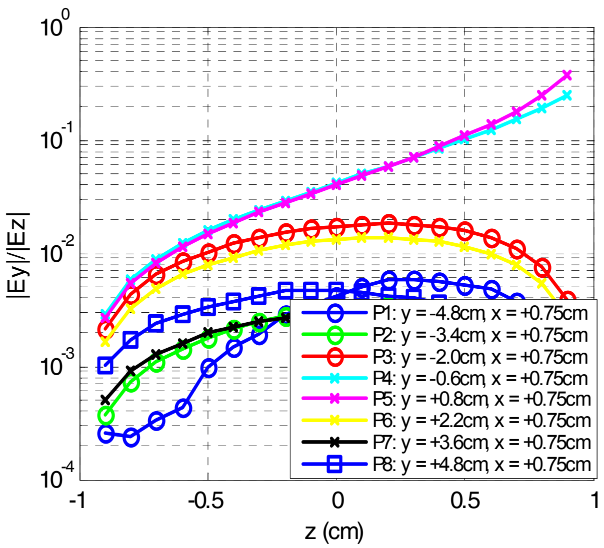

Fig.5. $|E_y|/|E_z|$ ratio as a function of z at 3.35 GHz for the 8 locations.

At the same time, the E_z-field component is not a constant any more when adjacent to the aperture. Fig. 6 illustrates the characteristics, showing the E_z-field as a function of z at different locations.

Fig. 7 further shows the E_z component values along the eight pre-defined lines for the cut plane at x = 0.75 cm. The E_z-field can be considered constant along all the lines but P4 and P5, which are under the aperture. Starting from z = 0.4 cm, the E_z-field starts to decrease along these two lines.

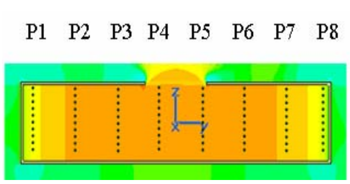

Fig.6. E_z field components at 3.35 GHz.

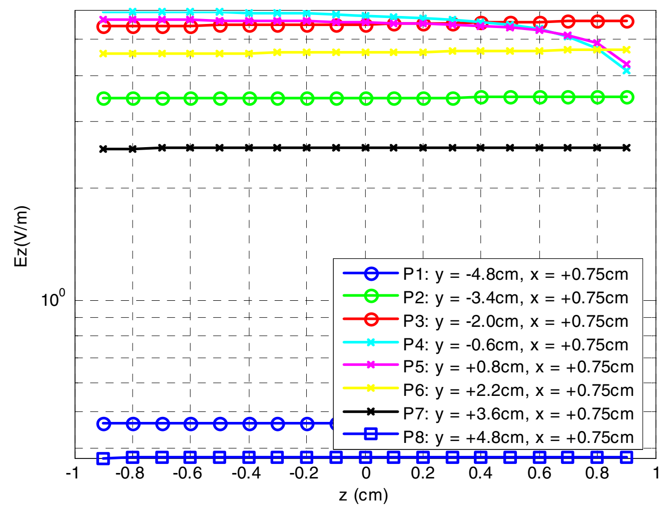

Fig.7. E_z as a function of z at 3.35 GHz for the 8 locations.

A percentage variation of the E_z-field along Line P_i (along the z-direction) can be defined as

$$\frac{\max\left|E_z\left(P_i\right)\right|-\min\left|E_z\left(P_i\right)\right|}{mean\left|E_z\left(P_i\right)\right|}\cdot 100\,. \qquad (2)$$

Fig. 8 shows the percentage variation of the E_z component for the same example data illustrated in Fig. 7. This parameter can be used to determine where the field variation due to the aperture becomes negligible, and thus PMC boundaries can be assumed again. The study herein is to model various cavity geometries with aperture using a full-wave method, and then to derive closed-form expressions of the percentage variation.

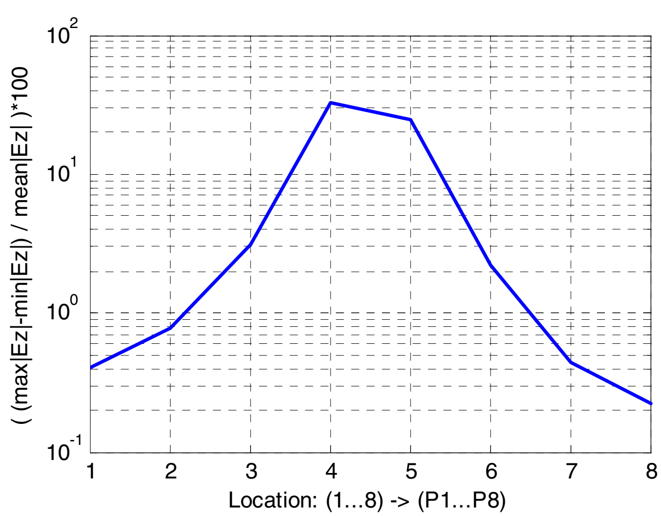

Fig.8. E_z percentage variation at 3.35 GHz for the 8 locations.

C. Full-Wave Modeling

Multiple test cases were simulated to derive the closed-form expressions using curve fitting. The geometry under study was a cavity with a square aperture in the center of the top wall. Three aperture sizes, 1x1, 2x2, and 3x3 centimeters, were investigated. The focus was put on the electric field computed inside the cavity at the first two resonant frequencies. Fig. 9 illustrates the simulation results for the three different aperture sizes at the first resonance (f = 3.35 GHz).

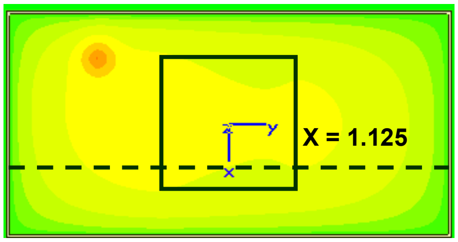

(a)

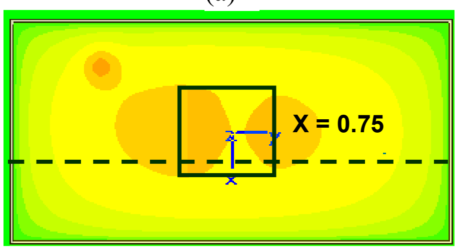

(b)

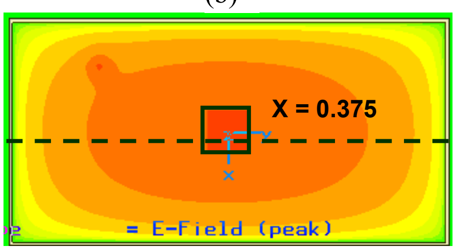

(c)

Fig.9. E_z distribution at 3.35 GHz for the cavity with a (a) 1x1, (b) 2x2, and (c) 3x3 cm aperture.

Field distribution was examined in a cross-sectional y-z plane (a cut plane, shown as the dashed lines in Fig. 9). The position of the cut plane varies so that the ratio between the spacing from the cut-plane location to the center of the aperture and the aperture size is 0.375. In other words,

$$\frac{x_{cut\ plane}}{aperture\ size} = 0.375 \tag{3}$$

Fig. 10a and Fig. 10b show the simulation results of the E_z-field variation along the cut plane at the first and second resonances, respectively.

III. Expression Derivation

A. Expression for a Square Aperture

A closed-form expression can be developed to approximate the E_z-field variation as a function of the aperture size and frequency, based on the full-wave simulations.

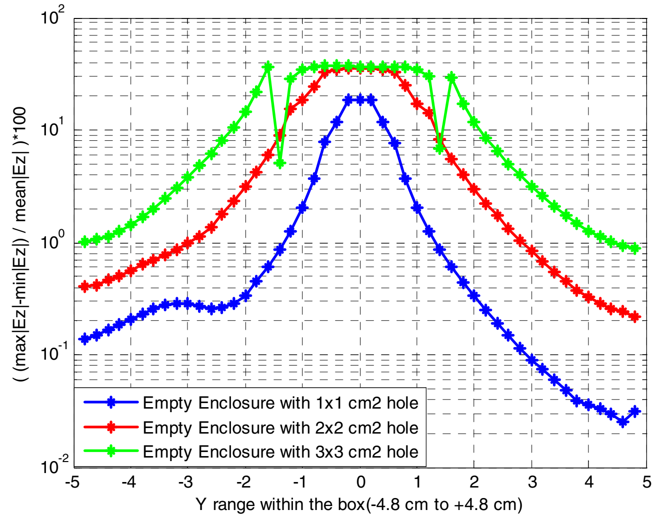

(a)

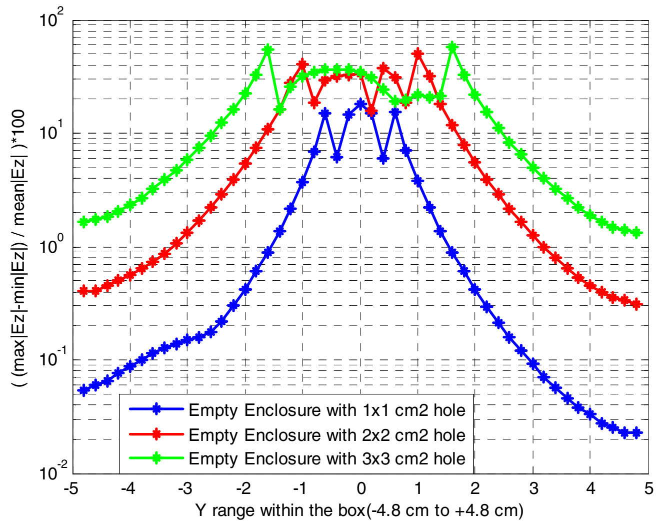

(b)

Fig.10. E_z field variation along the y-direction at the cut plane: (a) at 3.35 GHz; and (b) at 4.24 GHz.

As clearly shown in Fig. 10a and Fig. 10b, the E_z-field percentage variation decreases as a hyperbolic function when location moves away from the aperture. Based on this observation, a closed-form expression for a square aperture was derived by curve fitting as

$$\mathrm{var}(E_z) = \frac{A}{y} \tag{4}$$

where

$$A = 2 \cdot \frac{l_a}{\lambda_y}\left(10 \cdot \frac{l_{ap}}{l_a}\right)^{1.5} \tag{5}$$

The parameter A it is a function of the cavity length l_a, the aperture size l_{ap}, and the wavelength λ_y along the y-axes. λ_y can be calculated from (6).

$$k_y = \frac{m\pi}{a} = \frac{2\pi}{\lambda_y} \quad (6)$$

Where a is the cavity length at the y axis, and m is the mode number along the y axis for the given frequency. By including the wavelength, the frequency dependence in the approximation of the E_z-field variation is taken into account.

Since only the E_z -field variation outside of the aperture area is of interest, the portion of the data away from the edge of the aperture is used for the curving fitting, as marked in Fig. 11 using the dashed lines. Therefore the expression can only be used to estimate the E_z-field variation outside of the square aperture.

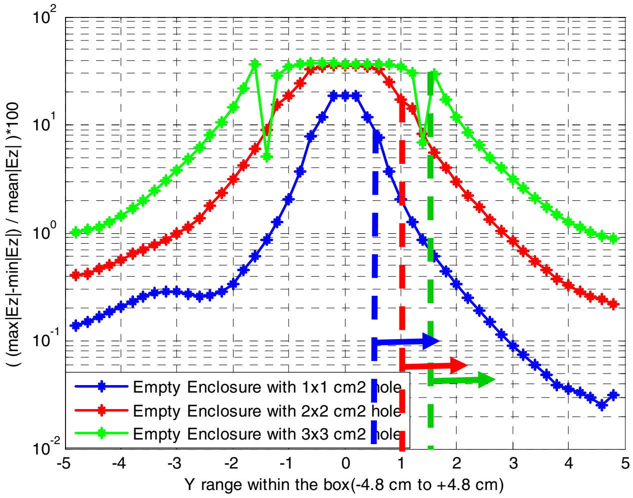

Fig.11. Limits of the data for extracting the closed-form expression; data at 3.35 GHz.

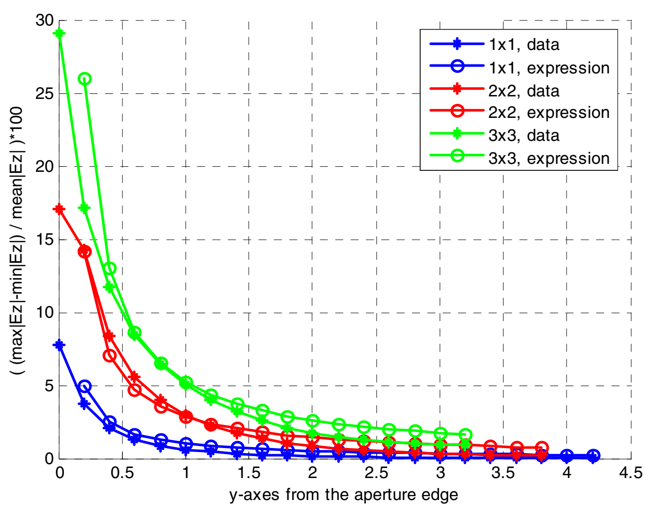

Fig.12. Validation of the closed-form expression at 3.35 GHz.

The closed-form expression has been validated with full-wave simulation results. The comparisons for the first resonance are shown in Fig. 12. As clearly shown, the expression can give a reasonably good approximation for the geometries under study.

Fig. 13 shows the validation of the closed-form expression at the second resonance. The agreement with the full-wave simulation data is generally acceptable as well.

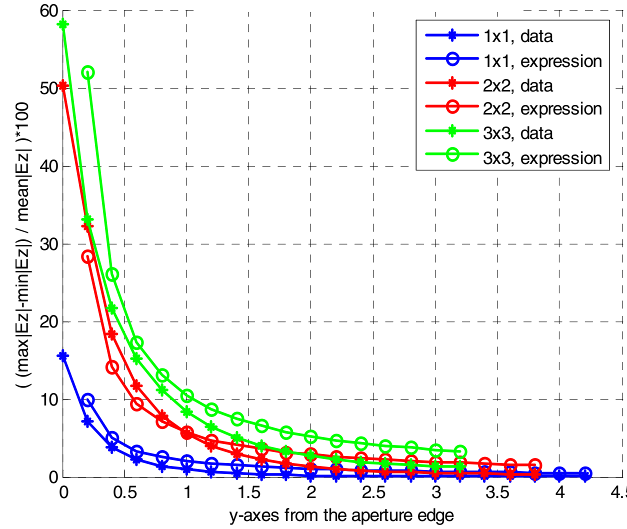

Fig.13. Validation of the closed-form expression at 4.24 GHz.

B. Expression for a Rectangular Aperture

The expression derived in (4) does not include the effect of the aperture dimensions when a non-square aperture is considered. An improved one was developed for a general rectangular aperture where the parameter A in (4) is

$$A = \left(\frac{l_{ap\_x}}{l_{ap\_y}}\right) \cdot \left(2 \cdot \frac{l_a}{\lambda_y}\right) \cdot \left(10 \cdot \frac{l_{ap\_y}}{l_a}\right)^{1.5} . \quad (7)$$

A new term, l_{ap_y}/l_{ap_x} is added as a ratio of the two aperture dimensions.

A new test case was investigated to validate the formula, with a 1x2 cm aperture in the center of the top wall, as shown in Fig. 14.

Fig. 15 shows the comparisons of the improved expression and full-wave simulation results along the y-direction at the first resonance for the new test geometry shown in Fig. 14.

The E_z-field variation calculated from the 3D simulation increases when the 1x2 cm aperture is considered with respect to the case of the 1x1 cm aperture. This behavior could be expected since the bigger aperture deviates more from the ideal field distribution in the cavity. Generally speaking, the agreement is very good, with the discrepancy in E_z-field percentage variation less than 2% for most of the cases. Some larger differences are found when close to the aperture edge, and especially for the biggest aperture (3x3 cm).

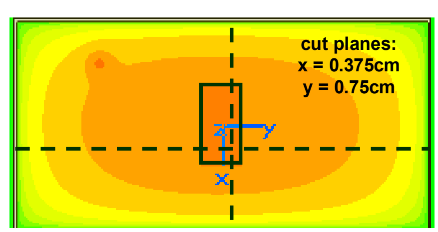

Fig.14. Enclosure with a rectangular aperture. The cut planes where the data from the 3D simulation are used are indicated as the dashed lines.

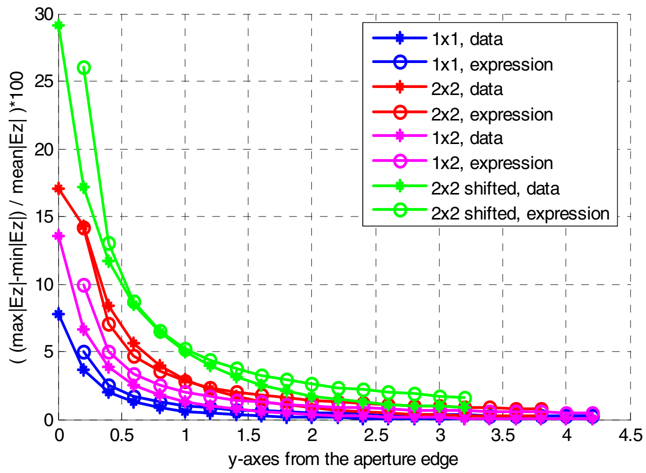

Fig.15. Validation of the improved closed-form expression at 3.35 GHz.

The E_z-field variation was also calculated along the x-direction at the x-directional cut plane shown in Fig. 14. The results are reported in Fig. 16.

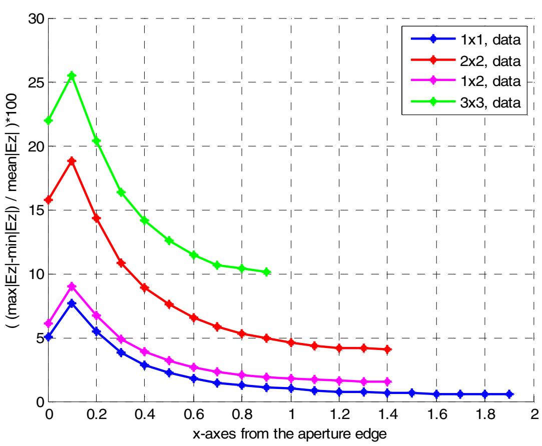

Fig.16. E_z-field variation along the x-direction.

The trend of the curves does not seem to match anymore with the hyperbolic approximation. This is due to the larger ratio between the aperture size (along the x-direction) and the cavity dimension (along the x-direction). In fact the difference increases with the increase of the aperture size.

The hyperbolic approximation as shown in (7) is modified to be applied to the E_z-field variation along the x-direction as

$$A = \left(\frac{l_{ap\_y}}{l_{ap\_x}}\right) \cdot \left(2 \cdot \frac{l_b}{\lambda_x}\right) \cdot \left(10 \cdot \frac{l_{ap\_x}}{l_b}\right)^{1.5}. \qquad (8)$$

The new results using (8) are shown in Fig. 17.

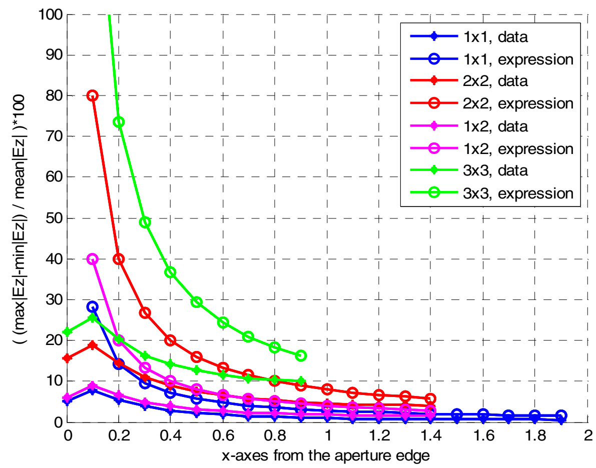

Fig.17. Validation of the improved closed-form expression at 3.35 GHz.

The agreement between the data from the 3D simulation is less satisfactory, as could be expected due to the high ration between the the aperture size (along the x-direction) and the cavity dimension (along the x-direction). In fact the values computed using (8) do not match those extracted from the simulation data for the 2x2 and the 3x3 cm apertures.

IV. Summary

Closed-form expressions have been developed to evaluate the E_z-field percentage variation when location is close to an aperture in a metal enclosure. The expressions take into account the effects of frequency, aperture sizes, and cavity dimensions.

The expressions have been validated with full-wave simulations. Good agreement demonstrates that the expressions can be used in engineering designs to estimate the field variations adjacent to an aperture, and thus to determine the PMC boundaries needed in the segmentation method.

V. References

1. Y. Zhang, X. Dong, Z. Yu, F. De Paulis, G. Feng, J. Mix, D. Hua, K. Slattery, and J. Fan, "Efficient prediction of RF interference in a shielding enclosure with PCBs using a general segmentation method," submitted to *EMC Europe 2008*, Hamburg, Germany, September 8-12, 2008.

2. T. Okoshi, Y. Uehara, and T. Takeuchi, " The segmentation method – an approach to the analysis of microwave circuits," *IEEE Transactions on Microwave Theory and Techniques*, vol. MTT-29, pp. 71-74, 1981.

3. G. Feng, G. Selli, K. Chand, M. Lai, L. Xue, and J. L. Drewniak, "Analysis of noise coupling result from overlapping power areas within power delivery networks," *IEEE International Symposium on Electromagnetic Compatibility*, Portland, Oregon, August 2006.